Minor Project

FEEDBACK FOR STABILIZATION DURING SWIMMING IN LAMPREY AND SALAMANDER ROBOTS

Patrick SANDOZ

patrick.sandoz@epfl.ch

June 10th 2011

Professor : Auke Jan Ijspeert

Assistant Supervisor : Jérémie Knüsel

Acknowledgments

The Minor Project in Biomedical Technologies proposed to Life Sciences Master students aims to immerse them into another multidisciplinary field of research to extend their skills and enlarge their area of interest.
The project that I performed in the BioRob Laboratory of Prof. Auke Ijspeert was a rich experience in terms of discovering new domains and expanding my abilities. I learned numerous new concepts and tools from robotic implementation and simulation to the different programming languages and the usage of LaTeX.

In consequence,

I would like to thank Professor Philippe Renaud for the organization and the support of the Minor program and for allowing me to perform this project related to Biomedical Technologies.

I would like to thank Professor Auke Ijspeert for his warm welcome to my application and for the trust he has given me to realize this project.

I would like to thank my supervisor Jérémie Knüsel for his important advices, his availability and his continuous support during my project.

I would like to thank Alessandro Crespi for his contribution for integrating the necessary material on the robot and for his explanations about the robot management.

Finally, I would like to thank Rolando Rodas for his precious help to improve my work, Jonathan Grizou for his continuous interest regarding this project and Steeve, Emilie, Andreas, Florin, Louis and Frederic for their support in my project.

Abstract

This project aims to study and provide a method of postural stability control for lamprey and salamander robots during swimming. The robot swimming gait is induced by a central pattern generator (CPG) distributed along the spinal cord. Up to now the robot stability was fixed using surfacing lightweight materials. This research has prospectively explored the possibilities to mimic the vestibular vertebrate system integrating acceleration sensing into the CPG network. It investigated the different limbs and tail movements relevant to produce stability and to correct mainly robot rolling and pitch tilt. Different simulations were performed in Webots^{TM} and then transferred to test the corrective effects of the network on the real robot. Progressive testing has provided sufficient information to discriminate efficient movements. The final implementation was tested during non-perturbed and perturbed swimming. However the last results were not significantly efficient compared to adequate controls. Nevertheless, the tests performed provided interesting information. It demonstrated that stability could be increased using the mentioned postural control method even if the new approach requires more tests and further investigations. The method was also extended to show the possibility of swim guidance in three dimensions. Thus this project has brought relevant approaches and it has opened a few new research questions and application.

Contents

List of Figures

List of Tables

This report is completed by a CD-ROM (on the back cover recto) containing the relevant simulation movies, the relevant movies of real tests on the robot, the source codes for the different parts of this project sorted in corresponding folders, the two presentations and the LaTeX source code of this report including relevant pictures.

1 State of the Art

1.1 Motivation

This project is concerned with lamprey and salamander robots of the BioRob laboratory. These robots are good anguilliform swimmers. Their swimming gait is generated by a central pattern generator (CPG) distributed in a double chain of oscillatory centres along their spinal cord [11, 10, 12, 2]. The swimming motion and the body oscillations producing the forward motion are planar.
However, in case of self-generated or external perturbations (created by forces and torques), inducing rolling, pitch tilt or yaw tilt, the swimming orientation changes and is no more corrected. The goal of the project is to find a method for postural stabilization against the different occurring perturbations. The method must have various characteristics like being adaptive to perturbation situations and inducing the use of a feedback control. The method should also be biologically inspired and based on the real animal shape and locomotion. Up to now, the orientation of the robot was maintained by keeping the robot at the surface plane with sagex pieces on girdles, thus avoiding any orientation change. Consequently the research area was very large and the orientation of the project may be progressively focused to restrain the domain to explore. From the beginning, yaw tilt was left aside to mainly try to counteract rolling and if possible pitch tilt (and yaw tilt is actually not a problem). Rolling is the most annoying perturbation because it prevents in particular tracking using the robot LEDs. This technique is required in some BioRob laboratory researches during swimming. Thus results of this investigation of a natural stabilization of the robot through the CPG will furthermore be directly relevant for further studies. Moreover, stable swimming enables also to decrease useless robot consumption of energy during tests.
Depending on the results, the postural control method might also be extended to guide the robot swimming, allowing it to change its swim direction, plunge or surface as required, and thus opening new horizons for its utility.

1.2 Literature Review

The biological inspiration is mainly retrieved from studies by Prof. Orlovsky and Prof. Deliagina's group (Karolinska Institutet, Sweden) on lamprey postural controls [7, 8]. In different publications up to 1992, they demonstrated successively that the postural controls in the lamprey integrate the animal's vestibular and visual systems to stabilize swimming against roll and pitch tilt [17, 6, 22, 19] and later on yaw tilt [13]. In particular, Kozlov et al. [15] demonstrated physically that a lateral flexion of the ventrally deviated tail, a lateral deviation of the dorsal fin and a body twisting would restore the initial orientation. The corrective

motion is induced from the reticulospinal neuronal pathway directly influenced by the ventricular and the visual pathways (cf. figure 1) [4, 6, 5, 20].

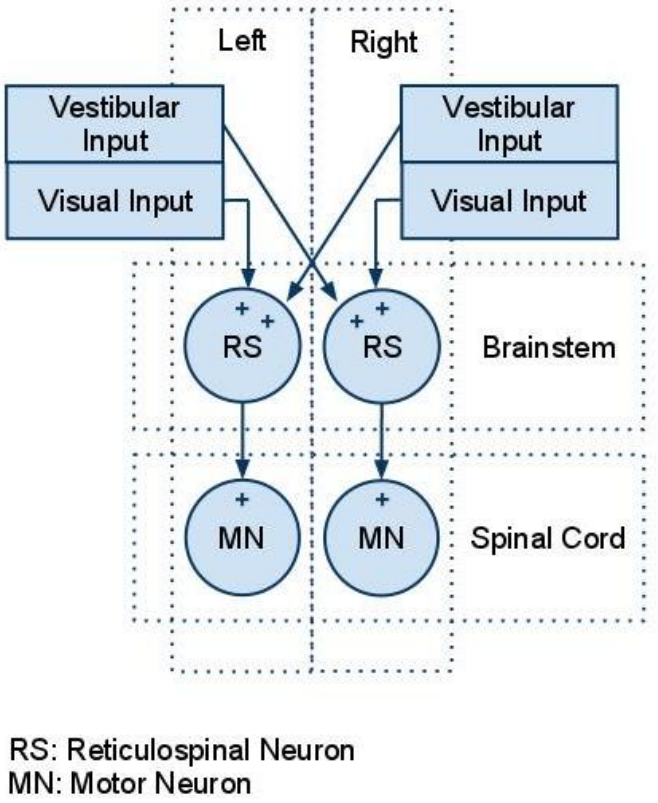

Figure 1: *Vestibular and visual systems induce a corrective a response to the spinal cord via a descending effective pathway [15]*

This postural stabilization method was thoroughly studied using labyrinthectomy and reviewed in the thesis of E. Pavlova [18]. Note that both sensing systems induce excitatory signals on the brainstem neurons and then downstream on the spinal cord neurons (contralateraly by the vestibular system and ipsilateraly by the visual system). Thus these descending signals acting from the mesencephalic locomotor region (MLR) to the motor neurons of the spinal cords until the most caudal segment corresponds to the descending command in our robots acting downstream on CPGs of the spinal cord.

If the stability of the salamander during swimming is almost not reviewed, the postural controls of fishes have been well documented by P.W. Webb [23] in *Fish Physiology*. The fish self-correction is a controlled dynamic state and dead fish dorsal side-up posture is clearly unstable. Fishes appear stable and highly maneuverable which is actually not the case of human engineered vehicles. They

mainly control three categories of perturbations to stabilize their body orientation, depth in the water column and trajectory. The abiotic perturbations are principally induced by gravity and wind-driven currents. The different perturbations are changing the location of the centers in the organism (center of mass and buoyancy centric height). The position of the fins relative to the centers of mass affects clearly the reactive effect. Note that the depth in the water column is regulated by gaz inclusion (in the swimbladder) even if it generates supplementary hydrostatic perturbations because the gaz volume is inversely proportional to pressure. The roll and pitch instabilities are produced by hydrostatic forces and might be corrected by hydrodynamic forces generated by the organism body and appendage movements. The fish head destabilizes in yaw, consequently it generally initiates turns and direction changes. The inertial state in water increases also these momentum. Finally different maneuvers exist like hovering, yawing turns, pitching, rolling and slipping. Note that anguilliform fishes are part of the most bending fishes (laterally and dorso-ventrally), enabling high body torques.

The state of the art in different autonomous underwater vehicle (AUVs) was also reviewed but little information on anguilliform swimming robot is available. Most interesting AUV were the lamprey robot of the Marine Science Center at Northeastern University [14] and the Snake-like ACM-R3 and ACM-R5 robots of Prof. Hirose's group in the Department of Mechanical and Aerospace Engineering, Tokyo Institute of Technology [16] which present both similar behaviours and locomotion patterns as our robots. However these robots are externally symmetric and they don't have a complete body stabilizing method. Note that the Snake-like robots immobilize the robot head from the neck joint to avoid unstable gait due to head integrated sensor movement [25]. Others AUV like the turtle of the Non-linear Systems Lab at Massachusetts Institute of Technology [21] or in the Aqua robot of the School of Computer Science at McGill University [9] use their limbs for swimming and stabilization. In the turtle robot case, the limbs have two degrees of freedom and use a combination of the two movements to act against rolling and pitch tilt. In the Aqua robot case, the robot is clearly not biologically inspired and uses three pairs of fins varying in amplitude and phase for swimming and stabilization. In summary, robots worldwide are currently using different methods for stabilization but none of these can be completely applied to stabilize our anguilliform swimming robots.

1.3 Movie Review

This project takes its source from biological mechanisms, so it was necessary to observe real animal life movements to truly understand the stabilization situation and process. Since salamanders are observable in nature only late in Spring and lampreys are a rare and protected species in Switzerland, this analysis was based on watching web movies. A list of interesting available movies with their references is presented in the appendices in the table 2. Different observations can be mentioned separating anguilliform limbless swimmers like the lamprey, eel, moray, sea snake (...) and anguilliform limbed swimmers like the salamander, newt, iguana, crocodile (...). Limbless swimmers seem to systematically correct their posture against rolling generating a torque relative to the longitudinal tail axis (the direction depending on the rolling side) and the dorsal fin has an important role to generate this torque accordingly to Kozlov et al. [15]. They usually keep their head motionless and generate the motion using only their body and their tail. The oscillation amplitude decreases from the tail to the head. Limbed swimmers seem to swim with body and tail oscillations and use only tail oscillation for fast gaits (for example in case of flight). For slow swimming motion and bottom walking, they use their limbs alternatively. Usually, during swimming they keep their limbs along the body and they deploy them to stabilize their posture when they stop. However quickly correcting with one limb is possible even during body oscillation.

1.4 Framework Orientation

These preliminary observations already produced a large framework of prospective research. In consequence the area of research was restricted to test a vestibular mimicking system integrated in the CPG network of the salamander robot inducing a postural corrective response using limbs and tail motions. All the tests were done on the salamander robot because it was more interesting to investigate corrective response using longitudinal body (which is implemented as the lamprey robot) and limbs motions. These motions were basically limited to the degree of freedom of the respective parts, (i.e. planar motions for the tail and rotational motions for limbs). Thus the postural stabilization method should be able to mainly correct rolling and pitch tilt. The salamander tail movement is restricted to lateral swipe. In consequence, the only variable parameters are the oscillation frequency and amplitude along the segment down to the more caudal one. On the other hand, the shape and the movement of the four limbs could be well adapted to respond correctly in terms of angular speed against a specific perturbation. Accordingly, it was decided to design simple limbs with new shapes, then to define angular speed profiles to generate different responses against per-

turbation and finally to implement them into the robot controller and test in a pool the postural control method.
The vestibular system furnishes to vertebrates with information on straight and angular accelerations. Because an accelerometer was already available to be implemented into the robot, it was decided to use this accelerometer to furnish the necessary orientation data to the controller and the CPG network.

1.5 Robot characteristics and Robotic Tools

This section shortly presents the characteristics of the salamander robot according to [3, 11, 10, 12]. The salamander robot was designed to study evolution changes, in particular aquatic to terrestrial locomotion transition. The robot consists of different modular segments (one head, two girdles with each a pair of limbs, six body segments and a tail). The gait is created by a central pattern generator (CPG) which is distributed longitudinally along the body in a chain of oscillatory centres. The resulting gait is an oscillatory motion at low frequency during walking and high frequency during swimming. While swimming, limbs were up to now inactive and kept along the body. The limbs motions are integrated into the CPG network and their response was linked to the body motion. Moreover the tail motion follows the descending body oscillation. Three models of tail were used. A short rectangular rigid tail, a short rigid ventrally deviated tail (as lamprey tail) and a long rectangular more flexible one.

Limbs

Four different limb shapes were retained to test their motion effect (see Figure 2). The first limb shape was the standard leg of the salamander that was used as an experiment control. The second shape was a palmed model of the leg (feet were enlarged). This shape should mimic fins and correct against rolling. The two last shapes were small and big ailerons (which should correct mainly pitch tilt). The small ailerons were retrieved from the laboratory material on a fish-like robot.

Accelerometer

Finally, a three axis digital accelerometer was integrated into the robot head by A. Crespi. Sensing acceleration on three directions enables to determine two of the three different cases of perturbation (roll and pitch tilt). The accelerometer was a MMA8453Q model of Freescale Semiconductor Inc. It was mounted on the I2C bus in the robot head. The accelerometer sensing is further described below in the chapter on calibration.

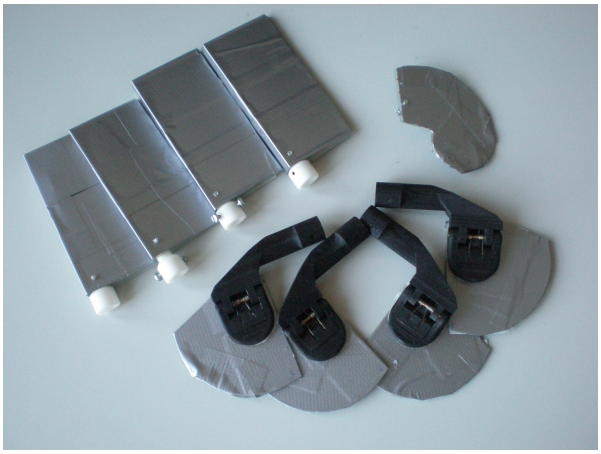

Figure 2: *Photography of the designed limbs, big ailerons and the ventrally deviated tail*

Robot weight

The robot produces a suitable approximation of the real salamander behaviour. However, a major difference resides in the weight to volume ratio of the robot. The real salamander has a variable ratio depending on the quantity of inspired air during the apnea. Expiration of a part of the air volume will also help the underwater animal to swim underwater. On the opposite, the robot has a fixed weight. The standard density of the robot makes it dive to the pool bottom. Thus up to now, the robot density was decreased adding low density material (sagex) to keep the robot on the surface and to stabilize it artificially. Before testing any corrective response, the robot density was adapted to obtain a water-close density which would let the robot dive to the pool bottom but also let it freely swim in the middle underwater zone. The density was corrected adding a smaller quantity of sagex that was fixed laterally on the segment (a location that does not artificially stabilize the robot).

Webots ^{TM} simulations

Various simulations were previously done using Webots software [24]. Fins were added and the physic plugin was completed with hydrodynamics of limbs. An accelerometer was also added in the robot head and the salamander weight was again also adapted (see Figure 3). The simulations tested the effect of limbs shape and movement from the initial perturbed situation. The correct weights of salamander segments, head, limbs and tail were added in the physic plugin of the salamander in Webots. However the balance of the salamander was not

appropriate (the salamander stabilizes in up pitch tilt situation because the head is lighter than normal segments and girdles). So the weights were adapted to test a model which stays stable underwater (the previous model corresponded only to the surfacing salamander).

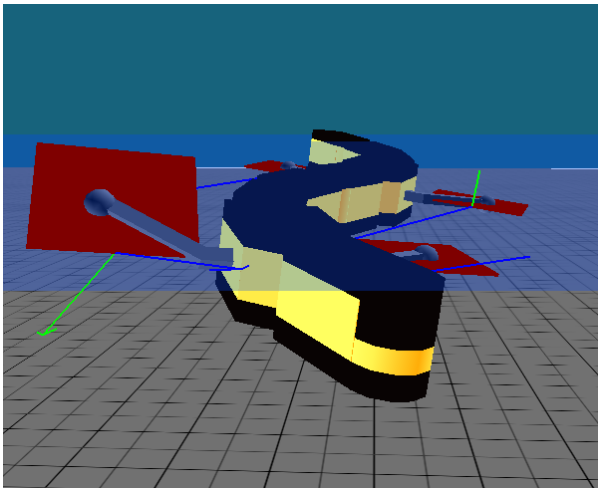

Figure 3: *Illustration of the robot simulation model. Green arrows represent limb force and blue arrows represents limb velocity*

2 Calibration and Implementation

2.1 Stability Definition

Stability definition is an important concept of this project. Up to now, the robot was kept on the surface by strongly decreasing its density with pieces of sagex. In consequence, important problems were avoided, such as weight imbalance of the robot disrupting swim guidance, also to prevent permeability of the module under water related to liquid pressure or still to avoid losing the robot in open water. This trick also averted roll over and pitch on the robot because the surface is a stabilizing environment.
In this project, taking advantage of the accelerometer sensor available, the stability is defined as the minimum of disruptive differences along the three axes of the sensor referenced to the gravity acceleration which is of course constant for every tested situation and so suits perfectly as a comparative variable. Nevertheless, swimming velocity has also to be considered, because stability has to be reached principally during swimming. For this purpose, acceleration measurements along the three axis were recorded for all the trials and velocity was determined measuring robot course with fixed trial duration. Acceleration measurements were retrieved and stocked in real time through robot radio communication.

2.2 Sensor calibration

Before any trial phase, the accelerometer had to be calibrated because the sensor was not oriented in the head as presented in the data sheet of the sensor. The MMAB453Q sensor is able to measures the acceleration reliably until twice the gravity on the three directions (the sensitivity is 256 counts/g). Thus the calibration was performed using the Earth's gravity as reference to identify the different axis of sensing. Different orientation recordings were performed. The acceleration was retrieved during 20 seconds at a recording frequency of 10Hz (this frequency was kept for all following tests). Four tests were sufficient to determine the sensing axis. These tests are presented graphically in Figure 4.
The first test presents the acceleration when the robot is flat and motionless. The retrieved signal is clearly unstable due to remaining small movements of robot segment even if the oscillatory amplitude is null. The second test presents acceleration during robot rolling of an half turn from left to right. The third test presents acceleration during robot down pitch tilt of a quarter of turn. The last test presents acceleration during yaw pitch tilt of a quarter of turn. These observations enabled to deduce the sensor orientation which is illustrated in the Figure 5.

Note that the motion acceleration induced on the robot during the trials was negligible compared to gravity and it was not increased to avoid robot damaging.

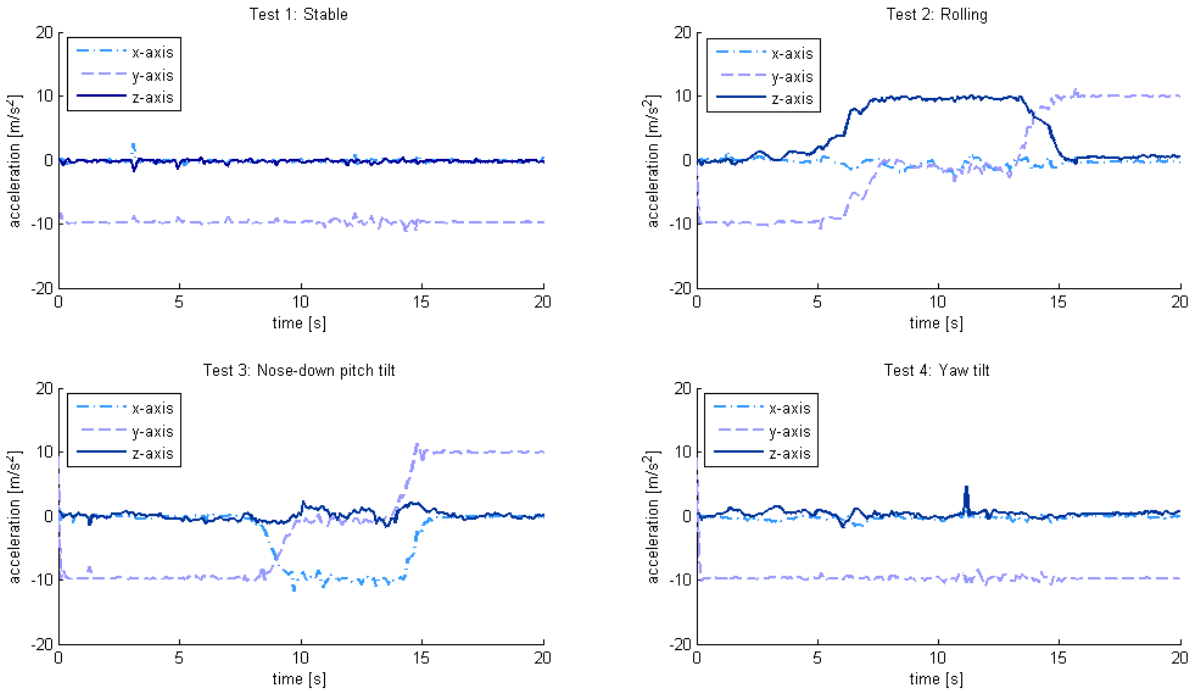

Figure 4: *Retrieved acceleration at 10Hz during 20 seconds tests for stable (upper left), half turn rolling (upper right), nose-down quarter turn pitch tilt (lower left) and yaw quarter turn tilt (lower right)*

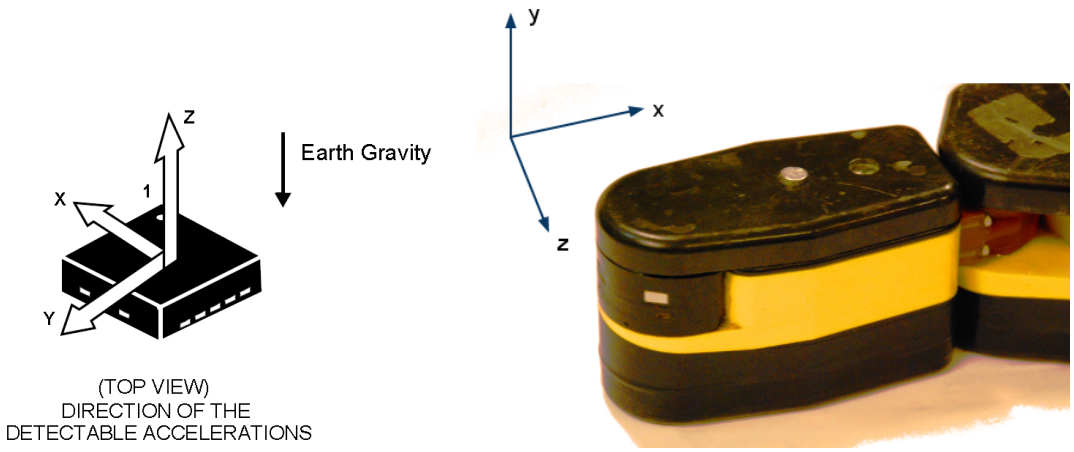

Figure 5: *MMAB453Q detectable acceleration (left) and sensing direction after the implantation in the robot head (right)*

We observed that the resulting signals can be analyzed in a perturbation case sensitive approach. However the different perturbations (the rolling, pitch tilt and yaw tilt) can only be defined precisely using the three recorded acceleration. Actually, a change in Y-axis acceleration can be indifferently caused by rolling or pitch tilt and only observing X-axis and y axis will provide sufficient information about the direction of the perturbation. The Table 1 below summarizes the particular cases.

Perturbation	X-axis	Y-axis	Z-axis
Rolling CW	Constant	Increasing	<0
Rolling CCW	Constant	Increasing	>0
Pitch tilt up	>0	Increasing	Constant
Pitch tilt down	<0	Increasing	Constant
Yaw tilt right and left	Constant	Constant	Constant

Table 1: *Limb and tail dimensions. The table is readable according to the accelerometer referential in the robot head. CW: clockwise. CCW: counterclockwise*

Note that the yaw tilt cannot be detected with this accelerometer using the gravity as reference (the accelerations into the robot oscillation plane are expected to be too low to be detected). Thus only the rolling and the pitch tilt case which are represented in the Figure 6 can be identified.

Figure 6: *Lamprey rolling (left) and pitch tilt (right) [18]*

2.3 CPG INTEGRATION

The central pattern generator network is an important tool to induce adaptive movements. Even if the network is provided to generate the body walking and swimming undulatory movement, the basic idea was to integrate stabilizing effects directly into the network. At the start of the tests, it appeared that stabilizing effects should be initially observed separately because it was not possible to discern corresponding reactions to perturbations.
Therefore, the network was integrated in several phases. Foremost, the different reactive effects were coded into the global controller through perturbation cases identifying and computational functions to update limb angles from acceleration sensing feedback. Tail specific reactions were initially ignored. Implementing the global control enabled to test the effects in Webots simulations before working on the robot. Thus at that moment, the limbs angles were directly written from the controller onto the CPG variables. Different profiles of angular speed response were generated using the program CPGStudio. The idea was to see how the motion of limbs in time will modify the postural equilibrium of the robot and thus correct it in a perturbed situation.
Here preliminary simulations showed that angular speed profiles were more or less similar due to the small amplitude of movement and the single degree of freedom. Thus, the basic chosen profile is represented in Figure 7.

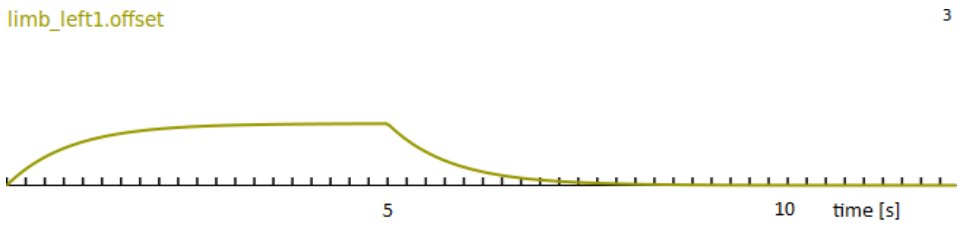

Figure 7: *Angular speed profile (offset) of a limb movement in time (back and forth)*

The implementation of the stabilizing model was also totally prospective. Apart from the reviewed marine turtle of MIT Marine department [21] (which used multiple degrees of freedom for the limbs and was not detailed in the articles), no previous studies were describing that kind of implementation. The first step was to define accordingly to the reactions observed in swimming vertebrates (on reviewed movies) which pattern will be relevant to be included. In this approach it was chosen to include in the implementation a case sensitive identification of the perturbations that will produce different counteractions. This computation was based on three variables updated with the sensed acceleration along their

respective axis. For the computation, different basic mathematic functions (like square root, arc tangent and arc cosine) were necessary. Then, the limb motion can be punctual to just react once to the perturbation or it can be periodic to try to correct the orientation longer. The periodic function was created from a cosine of the θ (oscillation phase) of the respective limbs (the θ is periodic and specific to the limb state, any other periodic variables were not usable because the time library is not available in the robot head controller). Finally, from the movie review, it appeared that swimmers slow down their gait when they have to correct their orientation, thus perturbed cases sensitive weights slow down the body oscillation amplitude when corrections are necessary. The model was firstly implemented as far as possible in the controller to observe the efficiency of the case sensitive computation. Then it was entirely transferred and improved into the CPG network to continue further tests (the tests are described in the chapter below about the tests on the robot).

3 Webots Simulation

3.1 Limbs various motions

Different limb motion types were investigated in simulation. However a hidden erroneous part of the hydrodynamic source code forced to remove angular forces of limbs during motion. In consequence, the movement of limbs did not correspond truly to the reality and indeed the movements observed later on the robot were different. Thus it was decided that most of the tests would be performed directly on the robot. Also, implementing perturbed cases of swimming into simulation would have been time costly while experiencing directly the perturbed swim on the real robot ensured results reliability. For these reasons, the simulations of limbs movement are not described here because the limbs reactive effects have remained irrelevant. Nevertheless, the limbs motion simulation in Webots was used to check the efficiency of the implementation to just induce any stabilization response. In this approach, punctual correction movements (as observed in the movies) and periodic movements (like fins correction in fish) were simulated in Webots and then transferred for tests onto the real robot.

3.2 Tail various motions

As mentioned before, simulations in Webots were performed preliminarily to real tests on the robot. These tests were used to observe behaviours and reactions in perturbed situations. However no statistically large simulations were undertaken.

First of all, it appeared globally that increasing the body and tail oscillation amplitude stabilizes the robot. Obviously, stationary objects are more perturbed because the required torque to induce rolling around the longitudinal axis is lower than for oscillating objects which increases the robot surface spreading.
Then, it seems that asymmetrical movements of the tail are not sufficient to counteract the rolling. The movement stays in the same plane as body oscillations and does not create a reversing torque. However without considering this problem of planar degrees of freedom, it is possible on Webots to modify the orientation of the rotating joints between the robot segments. Indeed, the simulation is no more representing the reality and these movements are not implementable on the robot, but it is interesting to observe while the tail oscillates perpendicularly to the body, that the movement stabilizes and counteracts the rolling. One simulation comparison is illustrated graphically in Figure 8. The graphic represents the rolling angle retrieved from the vertical acceleration sensing by trigonometry during 25 seconds. The simulation lets the robot start in a perturbed situation where the robot has already rolled over an angle of 45 degrees. The straight tail of the classic model is not stable and begin directly to roll over until stabilizing on the back (180 degrees) while the robot with a perpendicular tail induces more particular oscillations and stabilizes closer to zero. Note that the robot in simulation often stabilizes itself on the back. Reported simulation movies are available in *Results\Simulation Webots\Movies\Torques* on the attached CD-ROM.

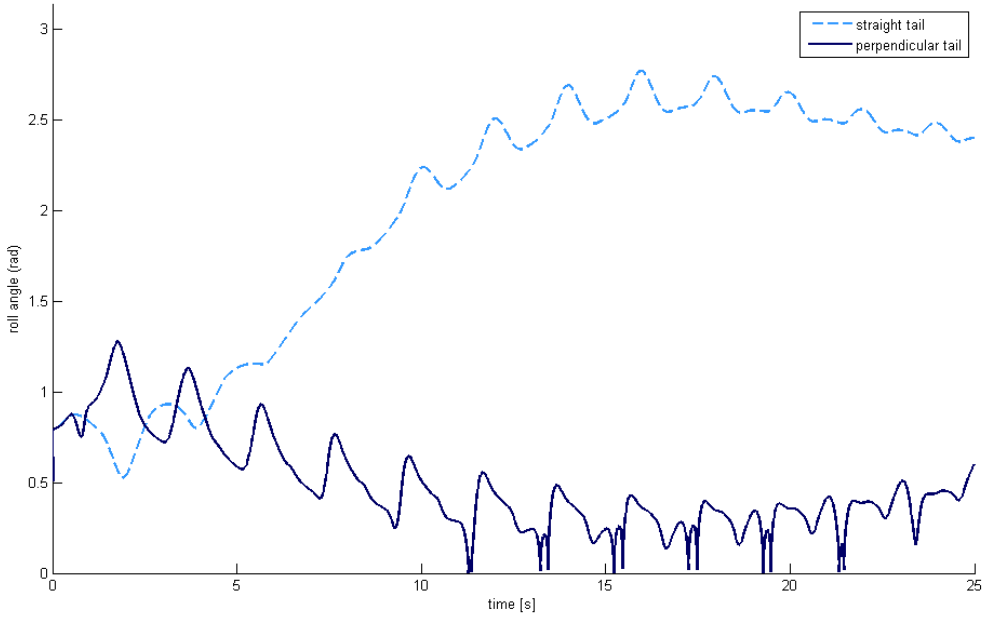

Figure 8: *Simulation comparison between straight tail and perpendicular non realistic but stabilizing tail motion*

4 Test on Robot

4.1 Limbs Tests

Different types of limbs were tested to determine which one will ensure from the beginning more stability during swimming. The limb types were the normal legs for walking, the designed fins, the designed big ailerons and retrieved small ailerons from a fish like robot model of the lab. The precise limbs dimensions are provided in Tables 3 and 4 in the appendices. Note that for all tests from here, the back girdle of the salamander had to be removed because its waterproofing was no more sufficient due to a broken leg rotor.

The limbs were mounted on the robot and the stability during swimming was tested during 20 seconds at different amplitudes of body oscillation (0.0m to 0.3m, from the center axis of oscillation). The maximum amplitude was only 0.3m because it corresponds to the amplitude needed to longitudinally cross the pool in the fixed laps of time. On the other hand, the oscillation frequency was fixed to 0.5 Hz because higher frequency would increase the speed of the salamander and it was expected that a high velocity might better stabilize the swimming and thus hide the tested movements. Boxplots of acceleration deviations along the different sensed axis are presented in Figures 19 to 23 in the appendices. From these data and in accordance to real time observations, it was decided to further use

the small ailerons which showed the better stability, keeping a sufficient speed (bigger limbs slow down the robot motion) and avoiding to regularly touch the pool bottom. Note that the pool is only 0.2m of water deep considerably reducing free movements.

The recorded accelerations along the three axes for the small ailerons tests are presented in Figure 9. Note that the test with amplitude set at 0.0m seems stable but only because the robot does not move and gradually touches the pool bottom. Then 0.1m amplitude is the most destabilizing swimming gait whereas amplitudes of 0.2m and 0.3m are almost similar (even if 0.2m is a little better). Increasing the longitudinal velocity and maybe also increasing the rate of the robot surface spread onto water basically stabilize against rolling.

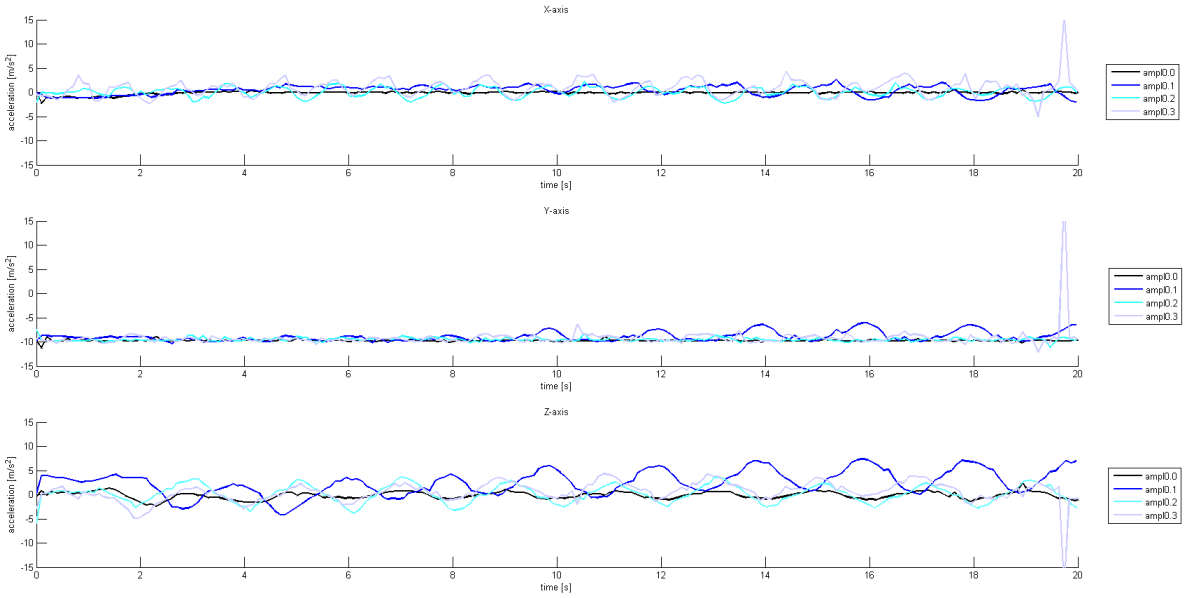

Figure 9: *Recorded accelerations for the small ailerons tests at various amplitudes*

At that stage of experiment, it was possible to test specific behaviours of the robot under ailerons motion. Two types of reaction were experienced. The first consisted in modifying both aileron orientations at a same angle to induce tilt movements (in order to use this movement against pitch tilt). Tests were performed along 20 seconds with an amplitude set to 0.2m, lowering ailerons of $\pi/3$ after 5 seconds and then raising the ailerons of $\pi/3$ after 10 seconds (angle zero reference is the longitudinal axis of the robot).
It was observed as expected that the robot firstly surfaced and stayed at the surface when ailerons were down and then the robot plunged and stayed underwater when the ailerons were up. A test example is available on the CD-ROM in *Results\Robot Tests\Movies\Surfacing*.
The accelerations along the three axis was recorded and is here represented in the graphic of Figure 10 with corresponding aileron angle orientation in time.

Note that the angle's sudden peaks are certainly recording errors.

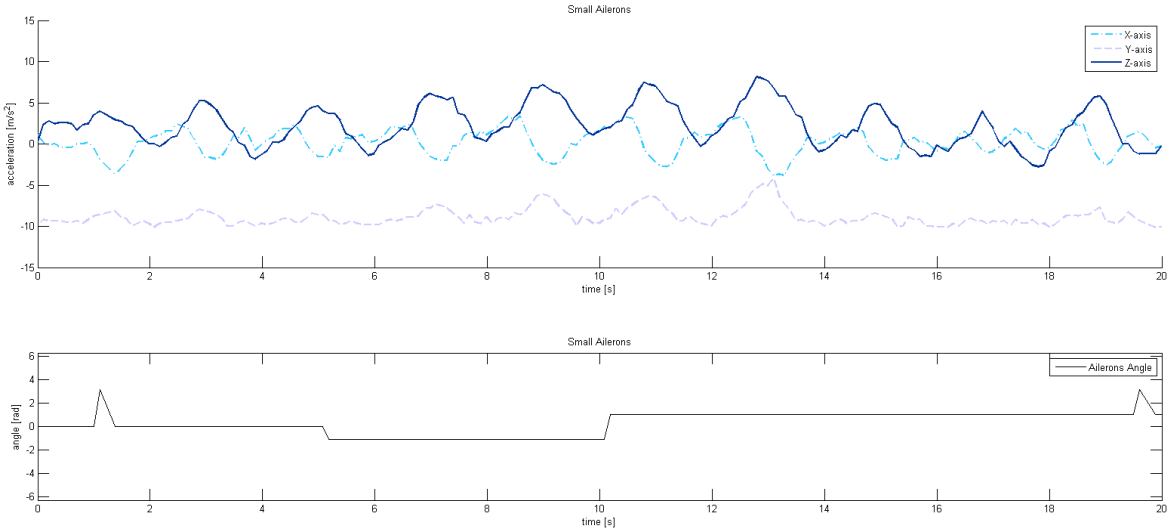

Figure 10: *Recorded accelerations for the small ailerons tests at various aileron angles*

The movie gives evidence that the ailerons have real effects even if the graphic in Figure 9 does not illustrate real impact of aileron turns. The reasons is that the robot orientation is not laterally perturbed and only pitch tilt is induced. However the pool is only 0.2m deep and the maximum tilt with a robot length of 0.75m to 1m (depending on the tail type) is between 10 to 15 degrees. So the recorded change of gravity in y axis is not inferior to 95%. On the graphics only a little change is observed after raising the ailerons at t = 10 seconds. Confirming the absence of rolling, the decrease of gravity sensed on the Y-axis corresponds to an increase of acceleration sensed on the X-axis.
Ailerons can also be used against rolling and for swim guidance opposing left and right aileron angles. Again, tests were performed during 20 seconds with an amplitude set to 0.2m, lowering/raising respectively the right/left ailerons of $\pi/3$ after 5 seconds and again inversing the angles after 10 seconds. The recorded accelerations for the two tested situations (left lowered first or right lowered first) are presented in the graphics of Figures 11 and 12.

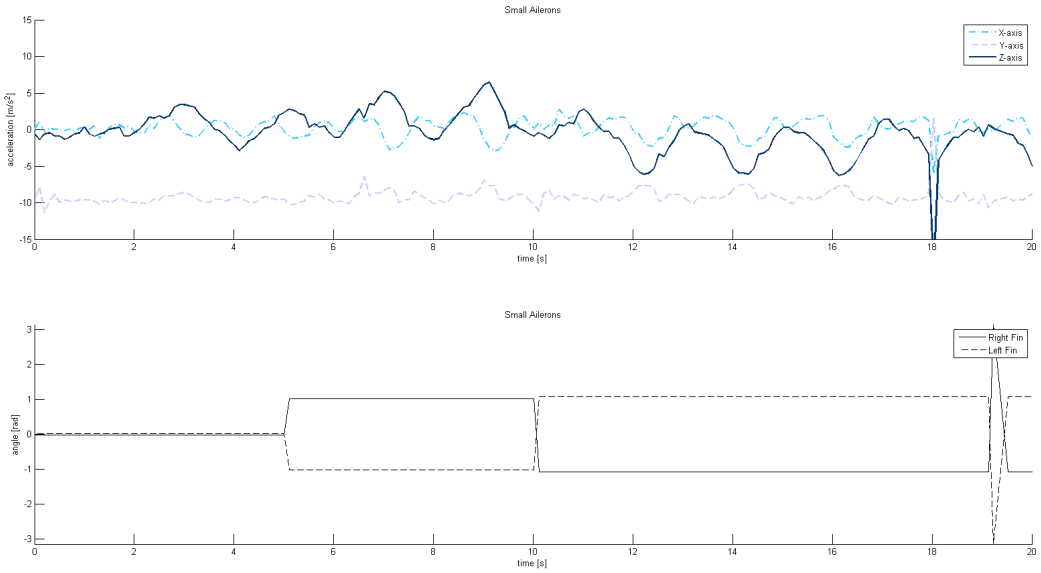

Figure 11: *Recorded accelerations for the small ailerons tests at opposed aileron angles, first case: left negatively, right positively*

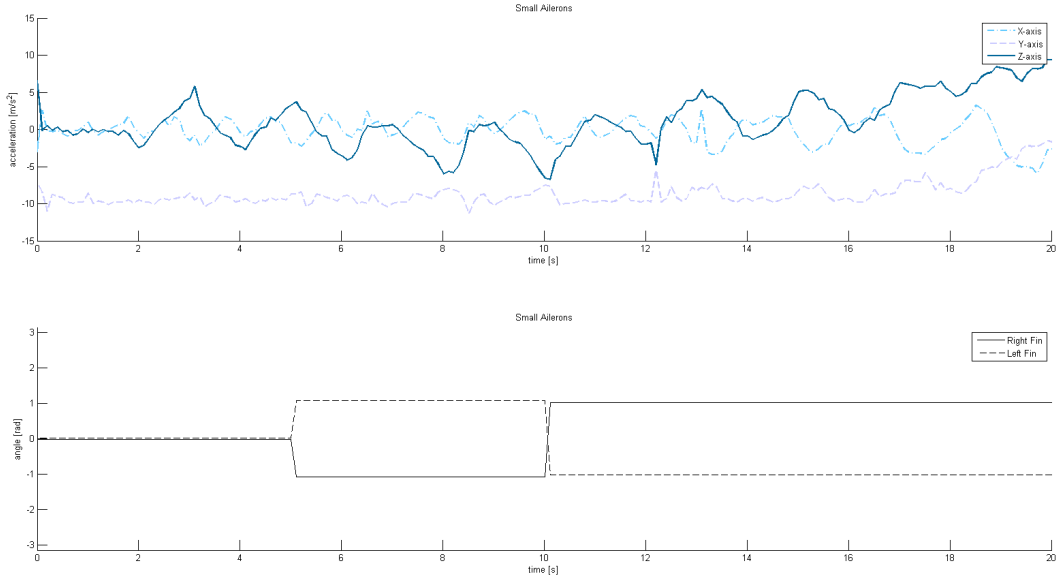

Figure 12: *Recorded accelerations for the small ailerons tests at opposed aileron angles, second case: left positively, right negatively*

Graphics show that the opposed rotation of the left and right ailerons induces a roll over effect bending the robot in the first case to the right after 5 seconds, then to the left after 10 seconds and inversely in the second case. Thus this effect could be used later to counteract rolling and further for swim guidance. These last tests are available on the CD-ROM in *Results\Robot Tests\Movies\Guidance*.

4.2 STABILIZATION DURING SWIMMING

Up to this point, the robot reactions were well defined and not adaptive to the real time situation. Using the different observations performed with well defined behaviours, a first adaptive model of stabilization was implemented in the controller (not yet in the CPG) and tested to see if the robot was able to identify the perturbation cases and adapt its movements consequently. An experiment, consisting of five repeated tests during 20 seconds of non perturbed swimming, was performed with small ailerons and an amplitude fixed at 0.2m. As previously mentioned, the distance swam by the robot is a complementary measurement of the stability, thus these distances were also noted. The boxplots of the absolute differences of recorded acceleration differences to the reference (zero for X and Z-axis and minus gravity for the Y-axis) is presented in Figure 13. A control experiment of five new tests was also performed with the same settings but without the adaptive model of stabilization. The boxplots of the control experiment are also presented in Figure 13 to be compared directly with adaptive results. The distances swam for the five tests of each experiment are also represented in the boxplots of Figure 14.

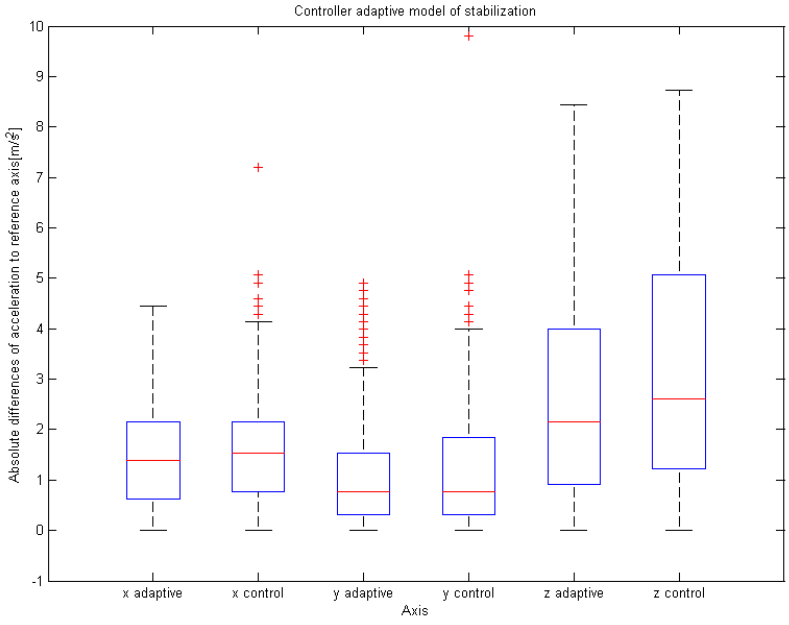

Figure 13: *Absolute differences of recorded acceleration differences for the tested adaptive model of stabilization into the controller during non perturbed swimming*

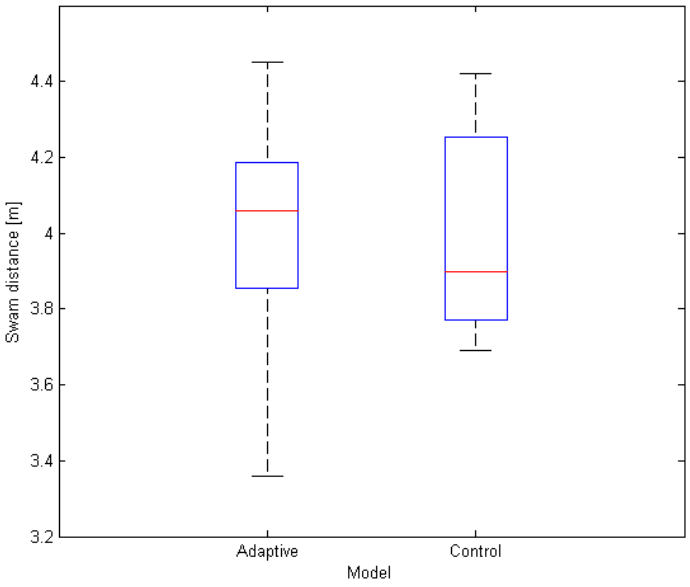

Figure 14: *Recorded distances swam for the tested adaptive model of stabilization into the controller during non perturbed swimming*

It appears clearly in the graphics that the benefits of the adaptive model is not significantly important even if the means are closest to zero for X and Z-axis and closest to minus gravity for Y-axis. The reason certainly is that the ailerons are already stabilizing the robot without specific movement while the constant oscillation of the head induced by the body oscillation inertia is inducing false rolling interpretation so the ailerons are mainly trying to counteract against the body motion and because no real perturbation is occurring, the difference is small. Even if the mean distance swam is higher for the adaptive model of stabilization into the controller, the difference compared to the control experiment seems not to be significant.
However, watching the movies (on the CD-ROM in *Results\Robot Tests\Movies \Adaptive*), it appears that the adaptive model mainly detects pitch situations and leaves aside rolling cases. In consequence, the pitch tilt is well corrected but not the turns.

Thus the idea was to test the adaptive model of stabilization in the controller, reducing the head movement. Here the technique of Prof. Hirose group where the snake-like robot head is stabilized canceling the undulation at the neck depending on the head direction and position [25] was not possible. The amplitude was simply reduced in the front girdle and in the first segments, maintaining oscillations only through the last segments and the tail. The same experiment was repeated and these results are presented as boxplots in Figure 15.

The stabilizing difference appears again really small due to the loss of surface

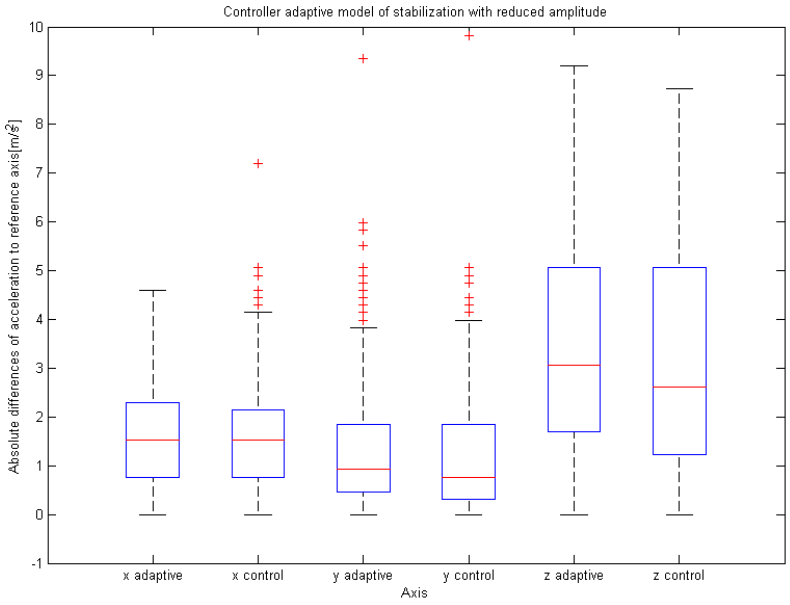

Figure 15: *Absolute differences of recorded acceleration differences for the tested adaptive model of stabilization into the controller during non perturbed swimming with reduced amplitude oscillation of the robot head*

spreading and the loss of motion at the front of the robot (we saw previously that the robot basically must move to stay stable). The push motion of the tail reduces the stability of the head and also reduces forward motion (the distance swam is lower: mean = 3.72m). So decreasing oscillation amplitude at the robot front is not a relevant solution.

Even if the adaptive model of stabilization in the controller seemed poorly efficient, the implementation was transferred into the CPG model allowing more possibilities of adaptation through the complexity of the network. The position of the limb defined by its angle was depending on the three acceleration components according to the rolling and pitch tilt detected situations. In rolling case, the limb movements were forced antagonist while in pitch case the limb movements corresponded to each other. The descending amplitude of oscillation was also decreased proportionally to the tilt. Then exactly the same experiment than the controller adaptive model was performed. The results for the CPG model of stabilization are presented in the boxplots of Figure 16 (the control boxplots are the same as previously).

The results show that the CPG model of stabilization does not add new benefits compared to previous observations. The results are similar to the controller model of stabilization with a high variability along the Z-axis due to the constant oscillation of the salamander robot body. The absolute acceleration differences

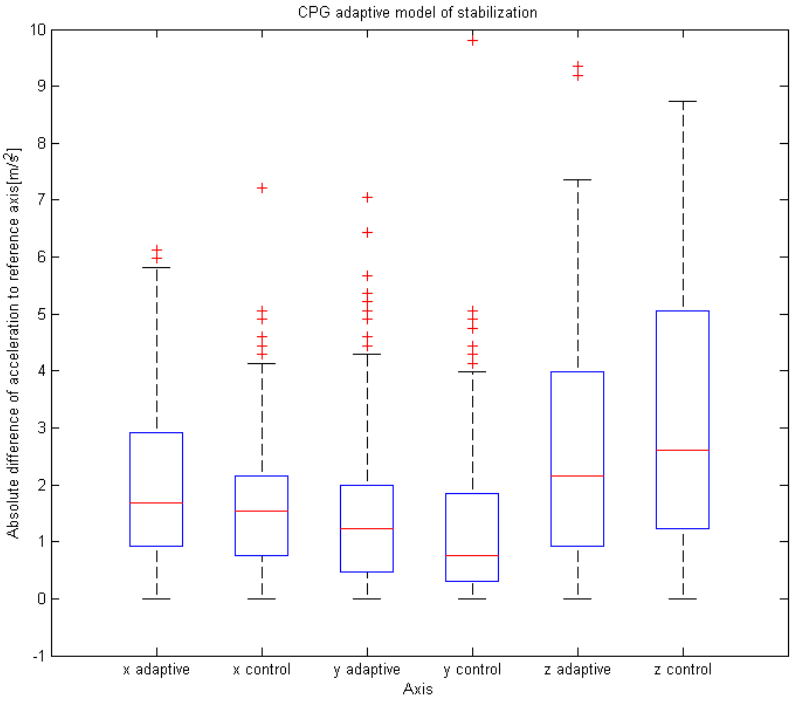

Figure 16: *Absolute differences of recorded acceleration differences for the tested adaptive model of stabilization into the CPG network during non perturbed swimming*

for the X and Y-axis appear for both implementations and for the control experiment already low and globally the variability is high. Further interpretations are presented in the discussion chapter.

4.3 STABILIZATION DURING PERTURBED SWIMMING

Previous tests have not shown important efficiency of the adaptive model for stabilization. However as explained earlier, it may be possible that the stabilization feedback induces continuous reactions because oscillations during swimming are producing regular changes of robot orientation that can be assimilated with perturbations by the network. To verify this hypothesis, complementary experiments were performed including a strong perturbation during robot swimming. Again five tests were done during 20 seconds with the small ailerons and a body oscillation amplitude of 0.2m. The distances swam were also recorded. The perturbation was introduced from the left side of the robot after 2m of swimming (corresponding approximately to 10 seconds) and consisted in a large wave inducing turbulences around the robot in the whole depth of the pool (most of the time the robot was deflected and turned. The results of this experiment are presented for the adaptive model of stabilization into the controller in Figure 17 and for the adaptive model in the CPG in Figure 18 (a new control experiment without movement was also done for the comparison).

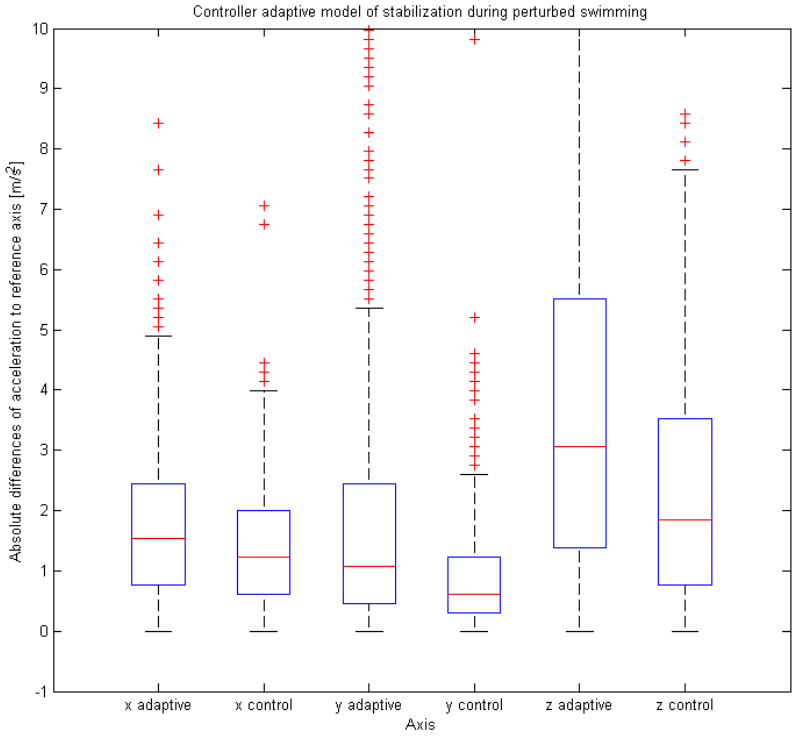

Figure 17: *Absolute differences of recorded acceleration differences for the tested adaptive model of stabilization into the controller during perturbed swimming*

Mean distances swam were 3.65m for the controller model, 2.53m for the CPG model and 3.92m for the control model.

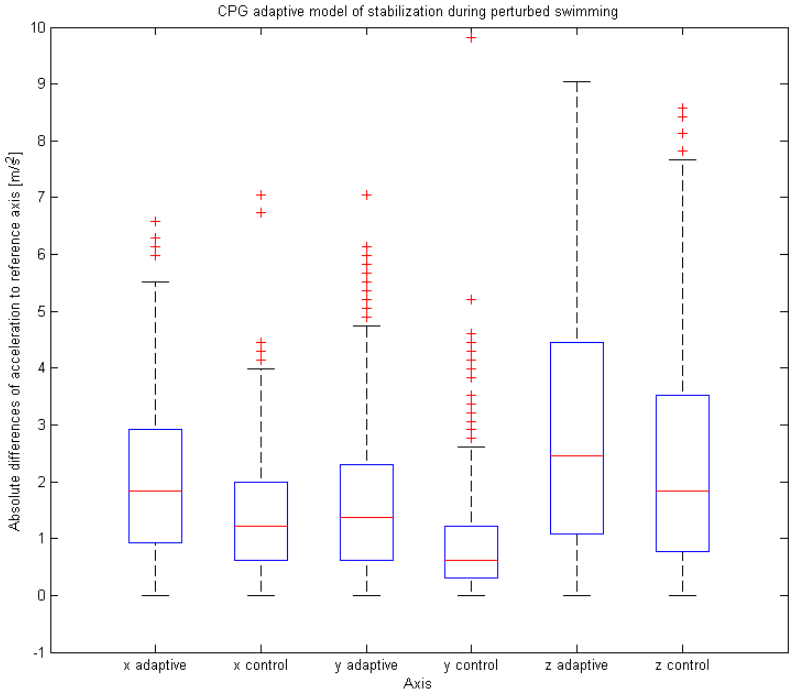

Figure 18: *Absolute differences of recorded acceleration differences for the tested adaptive model of stabilization into the CPG network during perturbed swimming*

Unfortunately, it seems that the CPG stabilizing model is also in this case not efficient. Note that the CPG model was still in attempting phase due to the numerous delays encountered during the project (these delays are described below). So reactive movements were mostly not well adapted and moreover perturbed the swimming. The comparison between distances swam showed also that the CPG model is less efficient than the controller model and the control experiment. Finally, the boxplots of Figure 18 are similar between the different stabilizing model implementations and the control experiment.
Note that synchronization of the CPG model is visible in the Figure 27 of the appendices on the Y-axis acceleration recording. These data show the same swimming pattern for the stabilization model (the starting swim position of the robot is always the same) but not for the control model whose only difference is the idle ailerons.

Note that during the controller model of the stabilization experiment, due to the perturbation induced by the wave, the robot turned on its back but the counteracting movement of the limbs redirected it correctly. However maybe the movement profited also of the echo wave (reflected by the pool edges). Unfortu-

nately this case was not observed during the control experiment avoiding any comparison. The graphics of these simulations are presented in the Figure 27 in the appendices.

4.4 TAIL VARIOUS MOTION

Different tail types were also used to investigate their stabilization potential. The types were a small tail of 9.0 cm, a long tail of 24.0 cm and a quarter circular deviated tail of 8.0 cm of radius. The different tails were alternatively mounted on the robot and the stability during swimming was tested during 20 seconds at different amplitudes (0.0m to 0.3m) of body oscillation. Accelerations along the three axes were recorded and the detailed results are summarized by boxplots in Figures 24 to 26 in the appendices.

Results showed that the ventrally deviated tail seems to ensure more stability along the three orientations compared to the straight small and long tails. However more tests during perturbed swimming would have been required but due the robot unavailability inducing at the end a lack of time, these tests were not performed. Note that for the limbs tests, the long tail was chosen because it was necessary to discriminate stability causes between the limbs and the tail (the ventrally deviated tail would have produce better results but leaving a bias doubt.

Finally, observing torsion movement of the tail would have been interesting because it corresponds with the stabilizing movement described by Kozlov et al. [15]. However creating these movements would have required to modify the rotation axis of the segment and that was obviously not possible. Thus tail oscillating movements were only tested in planar dimension.

5 Discussion

5.1 Results summary and further interpretations

Most of the results were described previously, however some global synthesis and interesting remarks can be added here. First of all the transfer of the simulated implementation to the real robot controller induced major differences of behaviour. Hydrodynamics in real environment is clearly different and the robot suffers more constant perturbations and orientation changes in the pool than in the simulated environment. The robot buoyancy is also dissimilar and adapting the robot weight is quite difficult in reality. Also, the accelerometer referential was available only chirally inversed in Webots compared to the MMA8453Q model. The progressive test phases enabled to be aware of the stabilization possibility depending on limbs and tail type and then to know the basic difference of stabilization during non-perturbed swimming.

These preliminary tests have shown that the small ailerons were the most adapted for the experiment, due to their more optimal size (bigger ailerons and limbs touch the pool bottom, whereas legs are not efficiently articulated decreasing any movement intensity). Since the orientation of the project focused on limbs movement, the tail asymmetrical movement were not investigated further than using Webots simulation but a simple experiment has shown that the ventrally deviated tail used is relevant basically just for swimming. The stabilization occurring with the ventrally deviated tail could be caused by the tail surface which is out of the profiled swimming hydrodynamic of the robot and maybe acts as a back ship drift.

Varying experimentally the amplitude of oscillation has shown that 0.2m is the best amplitude to test the robot. This result is in accordance with Jonathan Grizou project observation. To compare our results, he rescaled his observed natural salamander oscillation amplitude to the robot size and obtained also 0.2m. On the other hand, during the tests the oscillation frequency was fixed. It might be interesting in future tests to vary the oscillation frequency. The oscillation frequency is the natural way of the salamander to change its speed.

The various guided tests on limb movement types have shown that the limbs and particularly ailerons can clearly be used to guide the salamander. Raising both ailerons makes the robot plunge while lowering both ailerons makes the robot surface. Also opposing the rotation of the ailerons allows to turn right and left depending respectively on the angles on each side. However deploying the ailerons slows down the salamander robot swim and recovering the initial direc-

tion of the robot with the opposite limb movement was difficult.

The experiment of the stabilizing model implemented into the controller or implemented into the CPG was unable to produce some evidence of benefits of the reactive movements because the control experiment showed similar results of stabilization when the ailerons stay immobile. That could come from the fact that the ailerons deploy sufficient surface laterally to counteract most of the rolling effect. Also during non perturbed swimming, the case sensitive identification confounds the true perturbation with the normal oscillation of the robot which highly disrupt the acceleration recorded signal. This artifact could be corrected subtracting the self-generated signal components which are regular and known. As mentioned previously, the adaptive model in the controller detected mainly the pitch cases and left aside rolling cases, thus stabilizing correctly pitches but not turns.

Unfortunately, the experiment during perturbed swimming did not show evidence of any benefits of the stabilizing model apart the case where the robot was redirected after having turned back. However, the induced waves which produced the perturbations on the robot were generated by hand and so not always the same. Remember also that the CPG model due to the project delays was still in trial phases and many improvements and corrections can still be done. That's the reason why the planned test in big pool were canceled. Thus the laboratory pool was not the best environment to perform the tests because its depth was not sufficient to enable completely free swimming (limbs and tail often touched the bottom). The edges of the pool also reflected the wave during perturbed swimming experiments. The bio-inspired model is also limited by the robot shape. The natural salamander is flatter and offers more possibility of bending to decrease the torques that induces rolling.

Finally, graphics of the recorded acceleration have shown that the stabilizing model implemented in the CPG and in the controller have produced a kind of deterministic swimming gait which was adopted several times by the robot almost exactly during the tests. Thus the implementation seems to force the gait and maybe also reduce the adaptive possibilities of the robot during swimming.
Note that most of the interpretations were done without statistical computation. Principally because the number of tests was low due to the short remaining time available to test numerous variant models.

5.2 Encountered Problems

This section summarizes briefly the various problems encountered during the project and where possible it proposes solutions for improving the framework. First of all, this study was clearly prospective and it was planned to work mainly on the robot. However the research plan was modified several times due to unavailability and breakdown of the robot.

To start, the accelerometer sensor was unusable during the first eight weeks of the project and it was sent to be repaired, delaying the calibration phases and the initial tests. In parallel, simulation on Webots were not efficient due to a failure in the physics plugin which was part of the source code (and remains unsolved) and made simulation requiring periodic angular movements uncertain. Unfortunately, the pool for test on the robot was also unavailable during three weeks due to a leak. Then, most of the final tests were performed without the back girdles which had a broken legs preventing watertight sealing. Sealing was also a recursive problem. Modules frequently lost their waterproofing because tests required underwater movements like rolling or made the robot touch the pool bottom. At a time, it was considered to pack the salamander robot in a wet suit in theraband (a very elastic plastic film) that would maintain modules closed and increase the sealing. However, the plastic join was difficult and not convenient and the robot weight was no more adapted. It could be possible to fill the modules with hydrophobic non-conductive material to avoid water to enter.

6 Future Work and Conclusion

This study was mainly prospective and has covered many aspects of postural stabilization methods. Based on a literature review of the lamprey postural control and on limbed swimmer movies, stabilization recovery models were implemented. These models had led to different results from basic stability observations to complex reactive movements generated by the CPG network. Even if the final model is not efficient, progressive tests have shown small improvements of the stability. The use of an accelerometer to detect the orientation changes mimicked the natural vestibular system. However numerous tests can still be performed. Due to the setbacks during the project, the final CPG network was not completed and requires new experiments on the real robot to be improved. A less linear implementation could be created into the CPG, weighting directly the limbs movements and uniquely the tail from the front of the robot. The visual part of the vestibular system could be integrated using light sensor on the robot head even if the oscillating movement of the head might be perturbing. Also implanting a angular rate 3-axis gyroscope complementary to the accelerometer could simplify the identification of the perturbations (this system is actually used in above knee prosthesis to control the gait and the leg posture accordingly to the remaining leg [1]).
Modification on the robot could still be done. If the ventrally deviated tail brings more stability, it is possible that adding a dorsal or a ventral longitudinal fin will increase the stability against torques and rolling (acting as a drift). Stabilizing the head compared to the body would also reduce the acceleration sensing confusion. As mentioned before, these tests should be made in a deeper pool. That would improve the results quality and allow freer movements in any orientation of the robot.
Finally, even if many approaches could still be investigated, this project reached several objectives like assaying the potential of different postural stabilization controls being adaptive and bio-inspired. It brought many interesting reflexions, it required to work in many aspects of the robotic multidisciplinary domain and suited well as a translational area Minor Project.

References

[1] K. E. Akdogan and A. Yilmaz. Analysis of direct motion measurement system for design of above knee prosthesis. *IEEE*, 928(1):4244–5905, 2010.

[2] Alessandro Crespi and Auke Jan Ijspeert. Salamandra robotica: a biologically inspired amphibious robot that swims and walks. *BioRob internal review*.

[3] Alessandro Crespi and Auke Jan Ijspeert. Online optimization of swimming and crawling in an amphibious snake robot. *International Conference on Robotics and Automation*, pages 1513–1518, 2002.

[4] T. G. Deliagina. Vestibular compensation in lampreys: Impairment and recovery of equilibrium control during locomotion. *The Journal of Experimental Biology*, 200:1459–1471, 1997.

[5] T. G. Deliagina. Vestibular compensation in lampreys: Impairment and recovery of equilibrium control during locomotion. *The Journal of Experimental Biology*, 200:1459–1471, 1997.

[6] T. G. Deliagina, G.N. Orlovsky, and F. Ullen. Visual input affects the response to roll in reticulospinal neurons of the lamprey. *Experimental Brain Research*, 95:421–428, 1993.

[7] T. G. Deliagina and E. Pavlova. Modifications of vestibular responses of individual reticulospinal neurons in lamprey caused by unilateral labyrinthectomy. *Journal of Neurophysiology*, 87:1–14, January 2002.

[8] T. G. Deliagina, P. V. Zelenin, and G.N. Orlovsky. Activity of reticulospinal neurons during locomotion in the freely behaving lamprey. *Journal of Neurophysiology*, pages 853–863, 2000.

[9] C. Georgiades, Andrew German, and Andrew Hogue. Aqua: an aquatic walking robot. *Internal Review*, 2004.

[10] Auke Jan Ijspeert, Alessandro Crespi, and Jean-Marie Cabelguen. Simulation and robotics studies of salamander locomotion. *Neuroinformatics*, 3:171–196, 2005.

[11] Auke Jan Ijspeert, Alessandro Crespi, and Jean-Marie Cabelguen. From swimming to walking with a salamander robot driven by a spinal cord model. *SCIENCE*, 315:1416–1420, march 2007.

[12] Auke Jan Ijspeert, Alessandro Crespi, and Jean-Marie Cabelguen. Supporting online material for from swimming to walking with a salamander robot driven by a spinal cord model. *SCIENCE*, 2007.

[13] A. Karayannidou, P. V. Zelenin, and T. G. Deliagina. Responses of reticulospinal neurons in the lamprey to lateral turns. *Journal of Neurophysiology*, 97:512–521, 2007.

[14] T. Knutsen, Jim Ostrowski, and Kenneth McIsaac. Designing an underwater eel-like robot and developing anguilliform locomotion control. *NSF Summer Undergraduate Fellowship in Sensor Technologies, Harvard University*.

[15] A.K. Kozlov, E. Aurell, and S. Grillner. Modeling postural control in the lamprey. *Biological Cybernetics*, 84:323–330, 2001.

[16] M. Mori and Shigeo Hirose. Locomotion of 3d snake-like robots - shifting and rolling control of active cord mechanism acm-r3. *Journal of Robotics and Mechatronics*, 18(5):521–528, 2006.

[17] G.N. Orlovsky, T.G. Deliagina, and P. Wallen. Vestibular control of swimming in lamprey. i. responses of reticulospinal neurons to roll and pitch. *Experimental Brain Research*, 90:479–488, 1992.

[18] E. Pavlova. *Vestibular Control of Body Orientation in Lamprey*. 2004.

[19] E. Pavlova and T. G. Deliagina. Responses of reticulospinal neurons in intact lamprey to pitch tilt. *Journal of Neurophysiology*, 88:1136–1146, 2002.

[20] E. Pavlova, Lyudmila B. Popova, and Tatiana G. Deliagina. Vestibular compensation in lampreys: restoration of symmetry in reticulospinal commands. *The Journal of Experimental Biology*, 207:4595–4603, 2004.

[21] K. Seo, Soon-Jo Chung, and Jean-Jacques E. Slotine. Cpg-based control of a turtle-like underwater vehicle. *Auton Robot*, 28:247–269, 2010.

[22] F. Ullen, T. G. Deliagina, and S. Grillner. Spatial orientation in the lamprey. i. control of pitch and roll. *The Journal of Experimental Biology*, 198:665–673, 1995.

[23] P. W. Webb. Stability and maneuverability. *Fish Physiology - Fish Biomechanics*, 23(8):281–332.

[24] Webots. http://www.cyberbotics.com. Commercial Mobile Robot Simulation Software.

[25] H. Yamada, Makoto Mori, and Shigeo Hirose. Stabilization of the head of an undulating snake-like robot. *Proceedings of the 2007 IEEE/RSJ International Conference on Intelligent Robots and Systems San Diego, CA, USA*, pages 3566–3571, 2007.

7 Appendices

7.1 Detailed Results

Limbs movements

Here are presented the different results retrieved from tests on different limb types. The tests were performed during 20 seconds at different amplitudes of body oscillation. Boxplots summarize the experiment for each type of limb (legs, fins, small ailerons, big ailerons) and for the negative control (without any limbs). Boxplots were computed as acceleration deviation to zero for X and Z-axis and to minus the gravity for Y-axis.

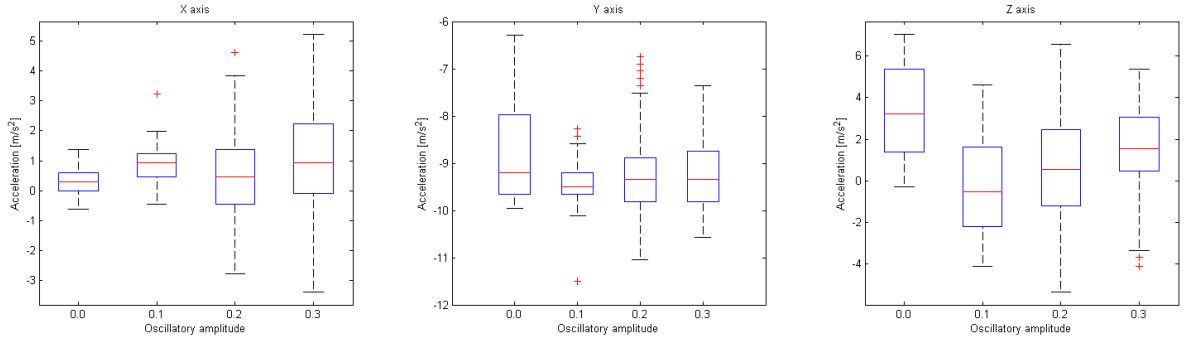

Figure 19: *Boxplot of acceleration during legs as limb test*

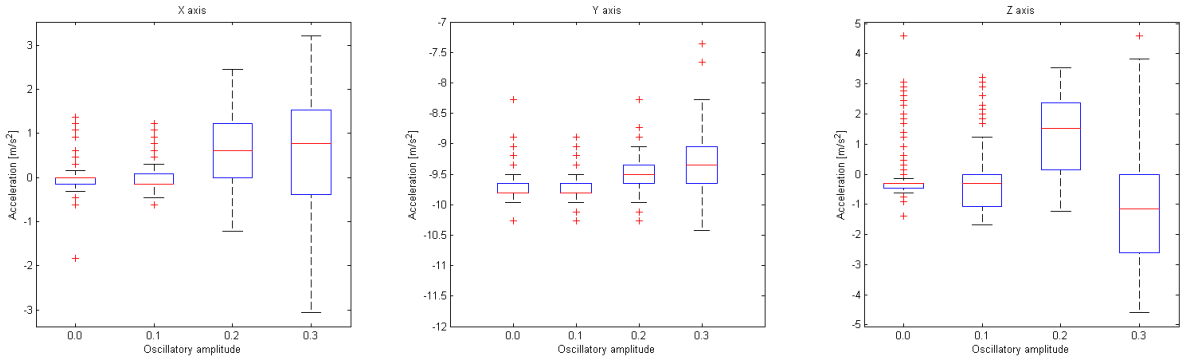

Figure 20: *Boxplot of acceleration during fins as limb test*

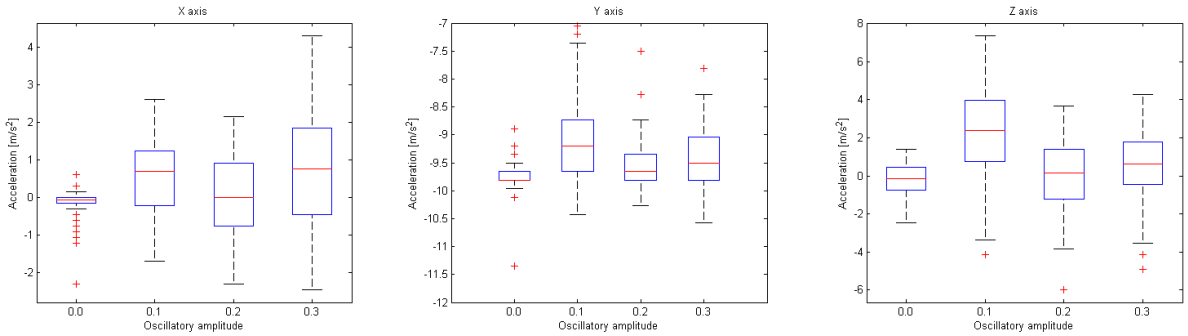

Figure 21: *Boxplot of acceleration during small ailerons as limb test*

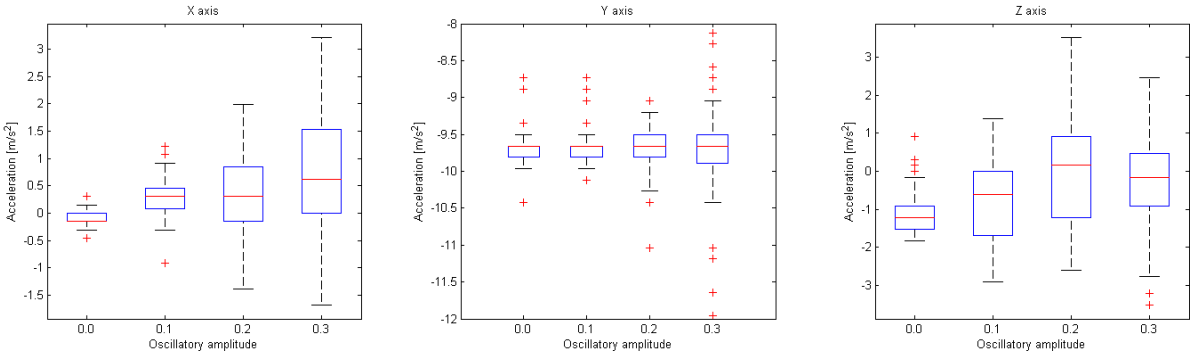

Figure 22: *Boxplot of acceleration during big ailerons as limb test*

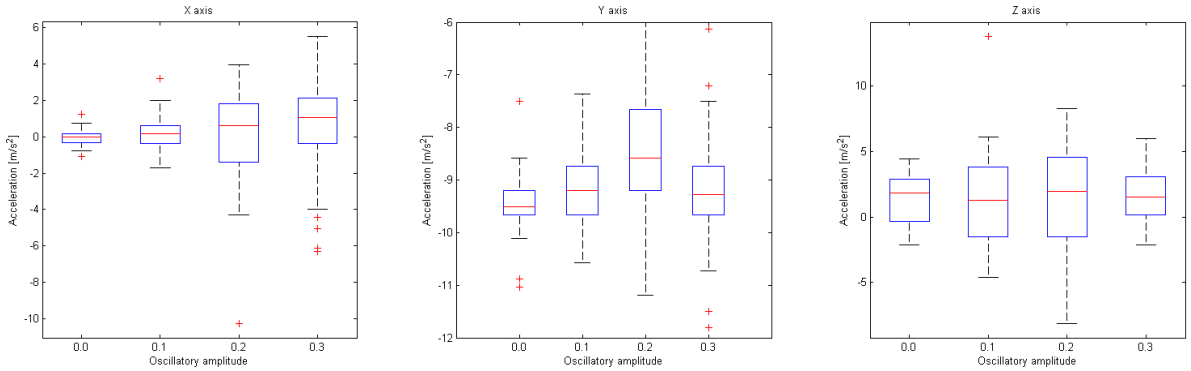

Figure 23: *Boxplot of acceleration during control test without limbs*

As explained previously in the results section, boxplots comparison allows to determine the most suitable type of limb. This limb should allow a very low deviation for Y-axis to ensure low rolling and low pitch tilt. Furthermore, a limb type that also reduces deviation in X-axis will be preferred (because it acts against rolling which is more perturbing than pitch tilt).
The boxplot analysis allows us to choose the small ailerons as limb type for the

further experiments because acceleration along X-axis and Y-axis are conserved more or less constant which is not the case for legs (X and Y-axis are less conserved), for fins (X and Z-axis are not conserved for high amplitudes), for big ailerons (again x and z axis are not conserved) and without axis (Y-axis is clearly not conserved). Note that for fins and big ailerons, the surface of the limb is too important slowing down the movement.

Tail movements

Here are presented the different results retrieved from tests on different tail types. The tests were performed during 20 seconds at different amplitudes of body oscillation. Boxplots summarize the experiment for each type of tail (small, long, and ventrally deviated). Boxplots were computed as acceleration deviation to zero for X-and Z-axis and to minus the gravity for Y-axis.

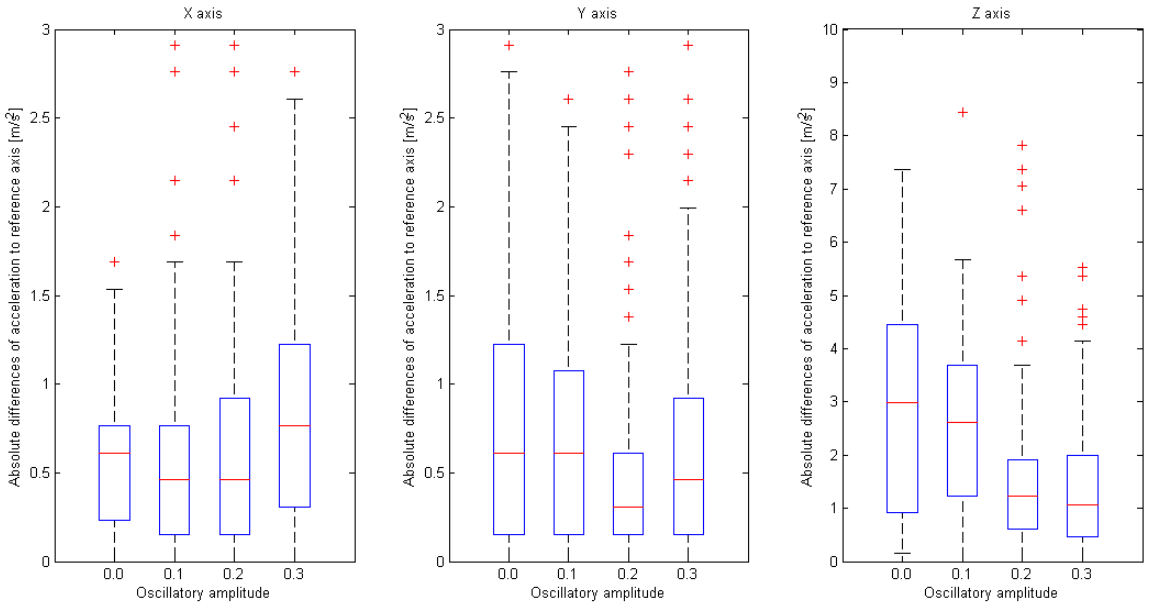

Figure 24: *Boxplot of acceleration during swimming with the ventrally deviated tail*

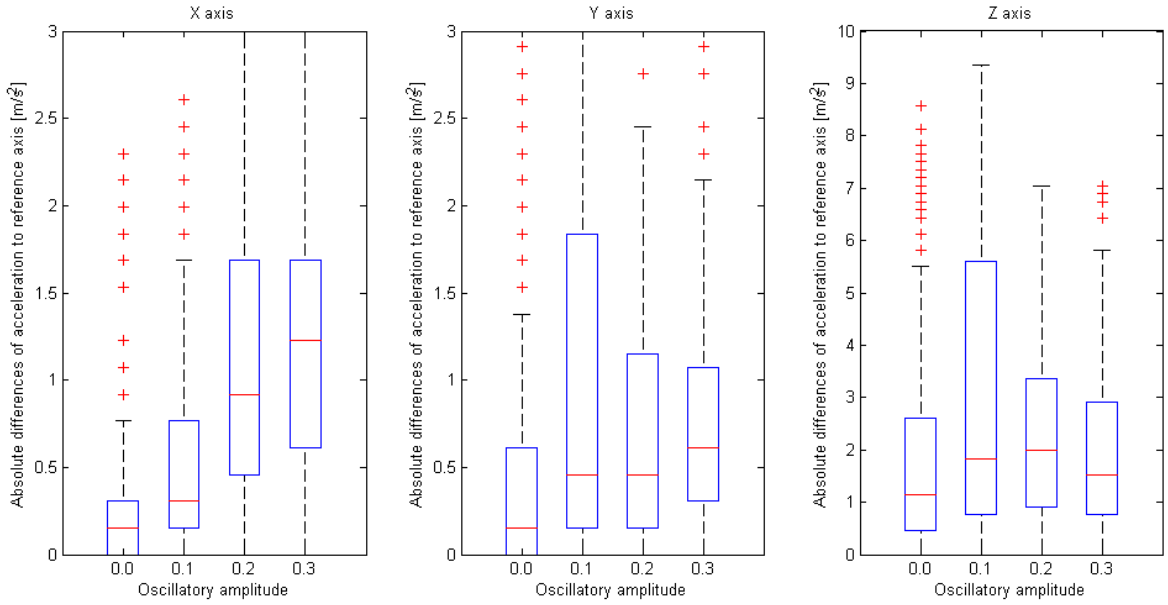

Figure 25: *Boxplot of acceleration during swimming with the small tail*

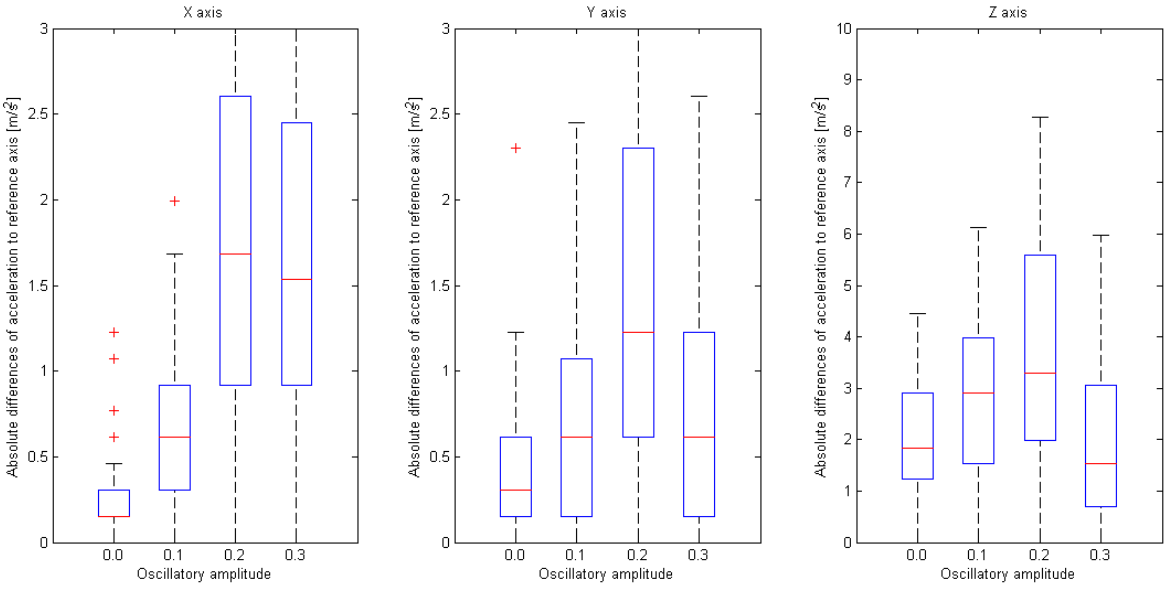

Figure 26: *Boxplot of acceleration during swimming with the long tail*

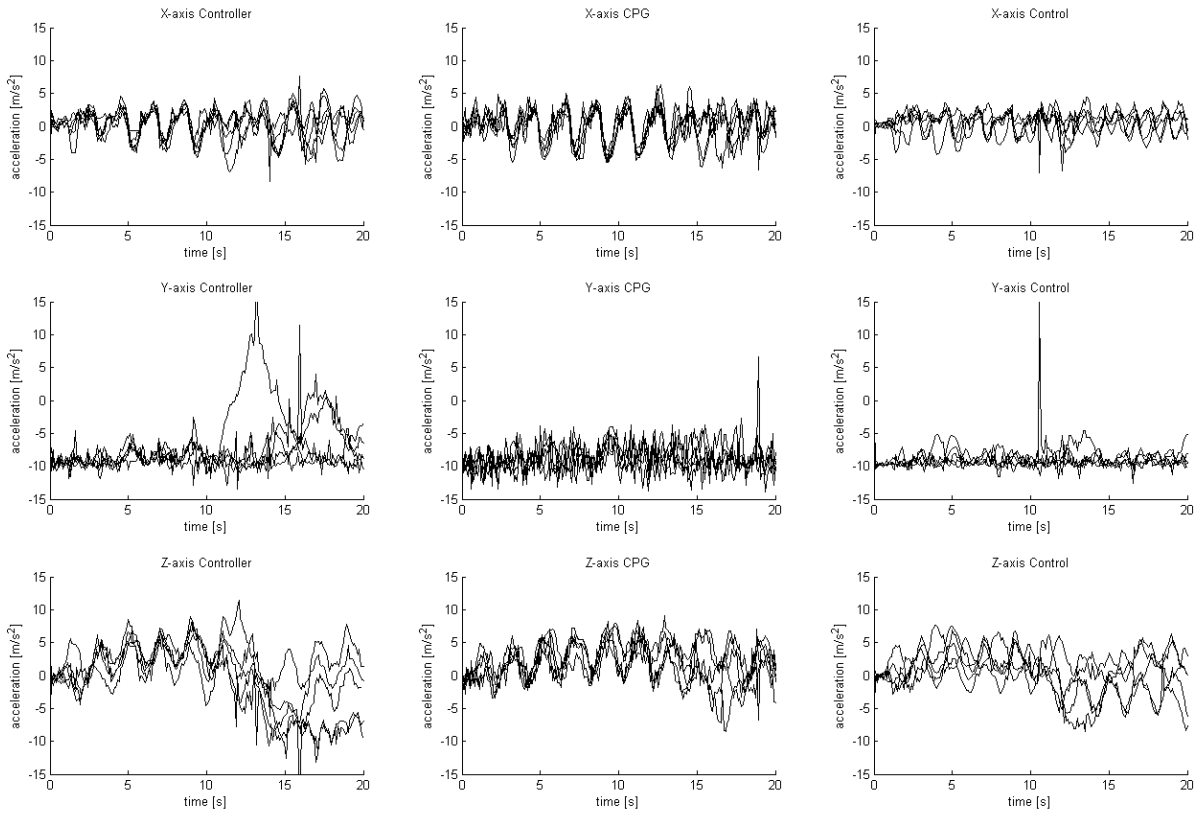

Figure 27: *Graphics of the recorded accelerations along the three axis during the perturbed swimming for the different adaptive stabilization models. The acceleration recorded when the robot has been turned back by the perturbation and then recovered its posture is visible on centre left graphic*

7.2 List of movies

Website	Animal	Environment	Time of interest [s]	Observation
2.1	Tiger Larvae	Nature	23	Limb deploying and correcting
2.2	Tiger Larvae	Aquarium	16	Limb correcting against rolling
2.3	Tiger Larvae	Aquarium	whole	Limb for small movements
2.4	Tiger Larvae	Aquarium	whole	retracting limbs to swim
2.5	Salamander	Aquarium	18	Pitch tilt up swimming
2.5	Salamander	Aquarium	42	Limbs retracting and deploying
2.6	Salamander	Nature	whole	Surface swimming with tail motion
2.7	Salamander	Nature	whole	Transition from walk to swim
2.8	Salamander	Nature	12	Tail motion oscillation higher than body
2.9	Salamander	Nature	0 to 10	Tail sufficient for swimming
2.10	Newt	Nature	0 to 10	Stop gait, limbs correction, tail asymmetrical correction
2.11	Newt	Nature	whole	Stop and deploy limbs to stabilize
2.12	Newt	Nature	whole	Stop and deploy limbs to stabilize
2.13	Newt	Nature	whole	Pitch tilt up stable with limbs
2.14	Newt	Nature	whole	Body and tail oscillation used in fast gait
2.15	Newt	Aquarium	whole	Body density higher than water
2.15	Newt	Aquarium	20	Surfacing to breath
2.16	Newt	Aquarium	whole	Limbs movement during swimming is possible
2.17	Lamprey	Nature	whole	Head on ground, asymmetrical tail correction
2.18	Lamprey	Nature	0 to 12	Asymmetrical tail correction
2.19	Eel\Moray\See snake	Nature	40	Asymmetrical corrective motion
2.20	Eel\Moray\See snake	Nature	whole	Head immobile and up pitch tilt
2.21	Eel\Moray\See snake	Aquarium	whole	Head immobile and only tail motion

Table 2: *Interesting movies descriptions*

2.1 - http://www.youtube.com/watch?v=F7gjIpNZbq4
2.2 - http://www.youtube.com/watch?v=ejiB7_d3vr4
2.3 - http://www.youtube.com/watch?v=goZmHSPrUUg
2.4 - http://www.naturefootage.com/video_clips/NZ26_071
2.5 - http://www.youtube.com/watch?v=MvqGQbtW0GA
2.6 - http://www.naturefootage.com/video_clips/MD01_086
2.7 - http://www.naturefootage.com/video_clips/MD03_029
2.8 - http://www.naturefootage.com/video_clips/MD03_005
2.9 - http://www.metacafe.com/watch/2286701/funky_zoo_103_funky_salamander
2.10 - http://www.youtube.com/watch?v=NOcLRkn7J-E&feature=related
2.11 - http://www.youtube.com/watch?v=Vg5f-KI4Rt4
2.12 - http://www.youtube.com/watch?v=aAD7y2jZtKg&feature=related
2.13 - http://www.youtube.com/watch?v=7-OG49J911o&feature=related
2.14 - http://www.youtube.com/watch?v=C7bXNpx3ZjU&feature=related
2.15 - http://www.youtube.com/watch?v=Mnw5kvix2JA&feature=related
2.16 - http://vimeo.com/groups/7286/videos/21725463
2.17 - http://www.youtube.com/watch?v=qxLeY8wP85k
2.18 - http://www.youtube.com/watch?v=wEkeHATroXo&feature=related
2.19 - http://www.youtube.com/watch?v=kr2PP23p384
2.20 - http://www.youtube.com/watch?v=gPj9gRZacPQ
2.21 - http://www.youtube.com/watch?v=2sadQUf2rD4

7.3 Limbs description

Type	Length [m]	Height [m]	Width [m]	Weight [g]
Small Tail	0.09	0.002	0.057	x
Long Tail	0.24	0.002	0.06	x
Ventrally deviated Tail	0.08	0.002	0.08	x
Legs	0.09	0.02	0.02	37.0
Fins	0.06	0.09	0.08	52.0
Small Aileron	0.06	0.002	0.04	15.0
Big Aileron	0.13	0.015	0.06	52.0

Table 3: *Limb and tail dimensions*

Type	Length [m]	Height [m]	Width [m]	Weight [g]
Head	0.095	0.057	0.045	185.0
Segment	0.095	0.057	0.045	220.0
Girdle	0.095	0.057	0.065	395.0

Table 4: *Robot module dimensions*